Biosensors and Bioelectronics 87 (2017) 495–500

Contents lists available at ScienceDirect

Biosensors and Bioelectronics

journal homepage: www.elsevier.com/locate/bios

Target-triggered catalytic hairpin assembly and TdT-catalyzed DNA polymerization for amplified electronic detection of thrombin in human serums

Kai Shi, Baoting Dou, Jianmei Yang, Ruo Yuan, Yun Xiang *

Key Laboratory of Luminescent and Real-Time Analytical Chemistry, Ministry of Education, School of Chemistry and Chemical Engineering, Southwest University, Chongqing 400715, PR China

ARTICLE INFO

Article history:
Received 27 June 2016
Received in revised form
14 August 2016
Accepted 17 August 2016
Available online 18 August 2016

Keywords:
Signal amplification
Electrochemical biosensor
Catalytic hairpin assembly
Thrombin
Terminal deoxynucleotidyl transferase

ABSTRACT

Specific and sensitive detection of protein biomarkers is of great importance in biomedical and bioanalytical applications. In this work, a dual amplified signal enhancement approach based on the integration of catalytic hairpin assembly (CHA) and terminal deoxynucleotidyl transferase (TdT)-mediated in situ DNA polymerization has been developed for highly sensitive and label-free electrochemical detection of thrombin in human serums. The presence of the target thrombin leads to the unfolding and capture of a significant number of hairpin signal probes with free 3′-OH termini on the sensor electrode. Subsequently, TdT can catalyze the elongation of the signal probes and formation of many G-quadruplex sequence replicates with the presence of dGTP and dATP at a molar ratio of 6:4. These G-quadruplex sequences bind hemin and generate drastically amplified current response for sensitive detection of thrombin in a completely label-free fashion. The sensor shows a linear range of 0.5 pM–10.0 nM and a detection limit of 0.12 pM for thrombin. Moreover, the developed sensor can selectively discriminate the target thrombin against other non-target proteins and can be employed to monitor thrombin in human serum samples.

1. Introduction

Thrombin, a specific serine endoprotease, plays a pivotal role in thrombosis, coagulation cascade, and hemostasis (Zhao and Gao, 2013). It is also an essential enzyme in different pathologic processes, including the development of Alzheimer's disease, leukemia and thromboembolic disease (Arai et al., 2006; Bauer and Rosenberg, 1984; Pabinger and Ay, 2009). Because of its important biological and clinical roles, the development of simple, sensitive and convenient methods for the detection of thrombin for diagnostic applications and clinical practice is thus highly desirable.

Aptamers are single-stranded oligonucleotides (DNA or RNA), which can bind specific targets such as proteins (Gao et al., 2015), metal ions (Mei et al., 2013), small molecules (Xu et al., 2014) and even whole cells (Liu et al., 2013) with high affinity and specificity. Aptamers are commonly obtained by in vitro systematic evolution of ligands by exponential enrichment (SELEX) process (Tuerk and Gold, 1990; Ellington and Szostak, 1990). Due to the synthesis convenience, easy and controllable modification, design flexibility and good stability (Lu and Willner, 2015), aptamers have been ideal recognition elements for the development of different types of aptasensors to detect thrombin. Typical thrombin aptasensors include fluorescent (Li et al., 2013), colorimetric (Huang et al., 2013), electrochemical (Du et al., 2014; Wang et al.,2014; Jiang et al., 2013b), and chemiluminescent sensors (Xia et al., 2015). Among these reported sensing platforms, the electrochemical thrombin aptasensor is a promising one because of its high sensitivity, quick response, low cost and portability (Zhang et al., 2014). In order to achieve high sensitivity, several signal amplification methods such as rolling circle amplification (RCA) (Jin et al., 2015), nuclease-assisted target recycling (Huang et al., 2015), polymerase chain reaction (PCR) (Yang and Ellington, 2008), and hybridization chain reaction (HCR) (Wu et al., 2015a) have been previously developed for sensitive detection of thrombin. Although these signal amplification methods are sensitive, the inherent limitations such as rigorous experimental conditions and unstable activity of enzymes became the issues in these sensing protocols. In an attempt to circumvent these limitations, the target-triggered catalytic hairpin assembly (CHA) has gained increasing interest because it overcomes the disadvantages of enzymatic amplification and avoids complicated techniques (Guo

* Corresponding author.
E-mail address: yunatswu@swu.edu.cn (Y. Xiang).

http://dx.doi.org/10.1016/j.bios.2016.08.056
0956-5663/

et al., 2015; Li et al., 2011). To further improve the sensitivity, many dual signal amplification strategies have been established for detecting the target molecules (Yang et al., 2013; Yang et al., 2015; Yu et al., 2016). Recently, a template-free DNA polymerase, terminal deoxynucletidyl transferase (TdT), which can catalyze the incorporation of multiple deoxyribonucleoside triphosphates to elongate the 3′-OH terminus of DNA and to consequently produce a tail, was explored as a new approach for signal amplification applications. For example, Tjing and co-workers (Tjing et al., 2011) have shown that TdT-mediated and surface-initiated enzymatic polymerization can significantly enhance the analytical signal to achieve highly sensitive detection of DNA or RNA targets. Most importantly, when a dNTP pool consisting of 60% dGTP and 40% dATP was used, TdT could then produce randomly arrayed G-quadruplex sequences (Liu et al., 2014), which bound hemin to form G-quadruplex/hemin complexes to generate amplified optical signal output. The primary advantage of this signal amplification method is that it does not require a specific secondary structure of aptamer, which is different from other non-label, DNA-based assays reported in previous work (Wu et al., 2015b; Qian et al., 2015) and can achieve label-free signal enhancement.

By taking the advantages of CHA and TdT-mediated DNA elongation amplifications, we report here a label-free and dual-amplified highly sensitive electrochemical aptasensor for detecting thrombin in human serums. The target thrombin molecules can trigger catalytic attachment of many hairpin signal probes on the sensor surface via CHA, and the 3′-termini of the captured DNA are then subjected to in situ TdT-mediated extension reaction to generate multiple G-quadruplex replicates with the help of dNTPs. These G-quadruplex sequences associate with hemin to form G-quadruplex/hemin complexes, resulting in significantly amplified electrochemical reduction current for highly sensitive detection of thrombin in a label-free approach.

2. Experimental section

2.1. Reagents and Materials

Thrombin, mouse immunoglobin G (IgG), lysozyme, carcinoembryonic antigen, 6-mercaptohexanol (MCH), tris (2-carboxyethy) phosphine hydrochloride (TCEP) and dimethyl sulfoxide (DMSO) were supplied by Sigma (St. Louis, MO). TdT was from Beyotime Biotechnology (Shanghai, China). Hemin was provided by Aladdin Reagents (Shanghai, China), which was prepared in DMSO to give stock solutions of 10 mM at −20 °C. Tris-HCl, deoxyguanosine triphosphate (dGTP), deoxyadenosine triphosphate (dATP), 4-(2-hydroxyethyl) piperazine-1 ethanesulfonic acid sodium salt (HEPES) and the oligonucleotides with sequences listed below were all ordered from Sangon Biological Engineering Technology & Services Co., Ltd (Shanghai, China). Thiol-modified hairpin immobilization probe (T-HP) containing the thrombin binding aptamer (Bock et al., 1992): 5′-ACA CCA ACC TTT TCG TTT TGG TTG GTG TGG TTG GAA TTT TTT-$(CH_2)_6$-SH-3′; Signal hairpin probe (S-HP): 5′-ACC TTT TCG TTT TGA CCA CAC CAA CCA AAA CGA AAA GGT TGG TGT TTC A-3′.

2.2. Preparation of the sensors

First, the gold disk electrodes (AuEs, 3 mm in diameter) were cleaned by immersing in the freshly prepared piranha solution (H_2O_2:H_2SO_4 =1:3, V/V) for 30 min in microcentrifuge tubes, followed by washing with deionized water. After that, the AuEs were polished step-by-step with 0.3 and 0.05 μm alumina powder on a flat pad for 5 min each to obtain mirror-like surfaces and were sequentially sonicated in deionized water and methanol for 5 min to remove any remaining impurities on the AuE surfaces. The AuEs were then electrochemically cleaned in a fresh H_2SO_4 solution (0.5 M) with successive scans from −0.3 to 1.55 V until remarkable voltammetric peaks were obtained. The AuEs were finally dried with a nitrogen stream.

The above AuEs were then incubated with 0.3 μM thermally denatured T-HP in 10 mM Tris–HCl buffer (1 mM EDTA, 10 mM TCEP, 1 mM $MgCl_2$ and 0.1 M NaCl, pH 7.4) for 12 h at 25 °C (Note: T-HP and S-HP solutions were denatured at 95 °C for 5 min and then allowed to cool down to 25 °C at a rate of 1 °C min^{-1} to stabilize the stem-loop structures). After washing with deionized water, the resulting T-HP modified AuEs were carefully dried under a stream of N_2 and then dipped into 10 μL of 1.0 mM MCH for 2 h to block the surfaces. After that, the sensor electrodes were rinsed with ultrapure water and dried with a stream of N_2 to obtain the T-HP/MCH /AuE.

2.3. Amplified thrombin sensing protocol

Ten μL of the working buffer (20 mM Tris–HCl, 100 mM NaCl, 10 mM KCl, and 10 mM $MgCl_2$, pH 7.5) containing various concentrations of the target thrombin and 1.0 μM S-HP were carefully dropped on the T-HP/MCH/AuE sensor electrodes and incubated at 37 °C for 120 min to obtain the S-HP/T-HP/MCH/AuE. After washing with buffer, 10 μL of the reaction mixture containing 1 mM dNTP (with a molar ratio of dGTP:dATP=6:4) and 10 U of TdT in the TdT buffer (25 mM Tris, 0.2 M potassium cacodylate, 1 mM $CoCl_2$ and 0.01% (v/v) Triton X-100, pH 7.2) was added to the sensor surfaces and kept at 37 °C for 1 h, followed by washing with buffer and incubating in 20 mM HEPES buffer (50 mM KCl, 200 mM NaCl, 1% DMSO, pH 8.0) containing 0.2 mM hemin for 30 min at 25 °C to allow the association of hemin with the G-quadruplex sequences.

2.4. Electrochemical measurements

A CHI 621D electrochemical analyzer (CH Instruments, Shanghai, China) was employed for all measurements. Cyclic voltammetry (CV) and differential pulse voltammetry (DPV) were performed by using a three-electrode arrangement: with a Ag/AgCl reference electrode, a platinum wire auxiliary electrode, and the modified working electrode. CV scans were performed in 0.1 M KCl solution containing 1 mM $Fe(CN)_6^{3-/4-}$ with a 50 mV s^{-1} scan rate from −0.1 to 0.6 V, and DPV measurements were carried out in 20 mM HEPES solution (50 mM KCl, 200 mM NaCl, pH 8.0) with the pulse amplitude of 50 mV, the sample width of 16.7 ms and the pulse width of 25 ms from −0.15 to −0.5 V (Note: HEPES solution was thoroughly degassed with N_2 for 30 min before the measurements).

3. Results and discussion

3.1. Design of the thrombin aptasensor

In the present work, target-triggered CHA is combined with TdT-mediated DNA polymerization to achieve dual signal amplification for sensitive electrochemical monitoring of thrombin. As illustrated in Scheme 1, the thiol-modified hairpin probes (T-HPs) labeled with thiol at their 3′ termini are immobilized on AuE surface via Au-S interaction. T-HP is designed to contain two functional sequences: the thrombin binding aptamer sequence (region I, the purple sequence) and the CHA initiation sequence (region II, the blue sequence) locked in the stem of TP. While, the signal hairpin probe (S-HP) contains a sticky end (region III) to hybridize with the CHA initiation sequence in T-HP. In addition,

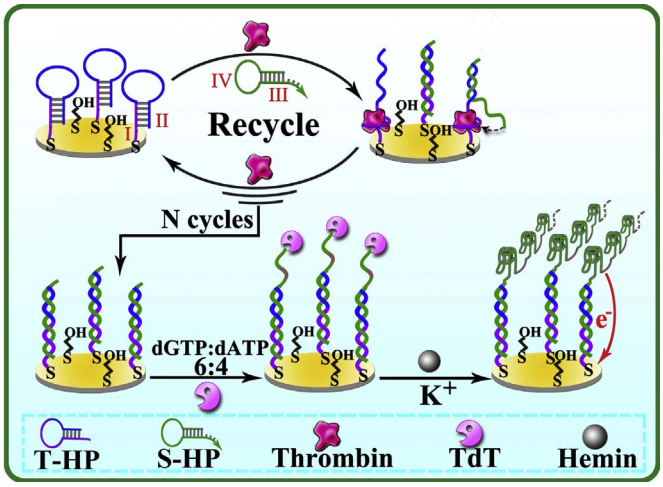

Scheme 1. Schematic diagram of the label-free and dual amplified electronic thrombin assay protocol based on target-triggered catalytic hairpin assembly and TdT-catalyzed DNA polymerization.

S-HP and T-HP are verified with the Mfold software to minimize their hybridizations with the folded hairpin structures (Zuker, 2003). In the absence of the thrombin target, the two metastable hairpin probes can coexist simultaneously, and the S-HPs can be removed from the sensor surface after washing with buffer. In such circumstances, the TdT-mediated DNA polymerization on the electrode is inhibited. On the contrary, when thrombin and S-HPs are incubated with the T-HP/MCH/AuE sensors, thrombin binds its aptamer sequence in T-HP (region I, the purple sequence) and unfolds the hairpin structure due to the high binding affinity between thrombin and the corresponding aptamer. Such binding leads to the formation of a free single stranded sequence (region II of T-HP, the blue sequence), which can hybridize with the sticky end of S-HP (region III) and proceed in a strand migration fashion (region IV) to hybridize with T-HP and to displace the thrombin target. The released thrombin again associates with the folded T-HP to initiate the CHA process, resulting in the hybridization of many S-HP with T-HP on the sensor electrode. The surface-hybridized S-HPs with free 3′-OH termini are further subjected to TdT-mediated DNA polymerization in a dNTP pool consisting of 40% dATP and 60% dGTP, which catalyzes repetitive addition of deoxynucleotide to elongate the exposed 3′-termini of the S-HPs and generates massive G-quadruplex forming sequences. Upon the addition of hemin and K^+, these in situ-generated G-quadruplex sequences bind hemin to form G-quadruplex/hemin complexes on the sensor electrode, and significantly amplified current response can be obtained due to electrochemical reduction of hemin to achieve highly sensitive and label-free detection of thrombin.

3.2. Electrochemical characterizations of the aptasensors

In order to characterize the stepwise modification process of the sensing electrode, CV measurements were performed in KCl solution (0.1 M) containing $[Fe(CN)_6]^{3-/4-}$ (1 mM) as the redox probes. As shown in Fig. 1, with the high efficiency of the electron transfer capability of $[Fe(CN)_6]^{3-/4-}$, the bare AuE exhibits a pair of well-defined, quasi-reversible redox peaks of $[Fe(CN)_6]^{3-/4-}$ (curve a). Dramatic decreases in redox currents (curve b) after the immobilization of T-HP and MCH onto the AuE surface can be observed because the DNA backbones are negatively charged and can repel the electrochemical probes, $[Fe(CN)_6]^{3-/4-}$, from accessing the electrode surface. After incubating the T-HP/MCH/AuE with the mixture of thrombin and S-HP, due to the steric hindrance effect of thrombin and CHA-induced formation of the

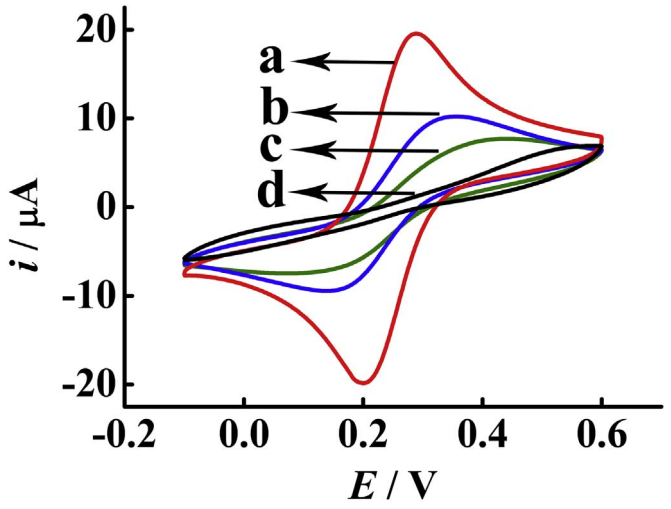

Fig. 1. CV characterizations of step-by-step modification of AuE: (a) bare AuE, (b) T-HP/MCH/AuE, (C) (thrombin + S-HP)/T-HP/MCH/AuE and (d) TdT/(thrombin + S-HP)/MCH/T-HP/AuE. CV scans were recorded in 0.1 M KCl solution containing 1 mM $K_3[Fe(CN)_6]/K_4[Fe(CN)_6]$ in the range from −0.1 to 0.6 V with the scan rate of 50 mV s^{-1}.

dsDNA on the electrode, further decreases in peak currents are obtained (curve c vs. b). Moreover, subsequent TdT-mediated DNA polymerization leads to almost the disappearance of the current peaks (curve d) because of the introduction of the elongated DNA sequences on the electrode, which significantly increases the negative charges and steric hindrance to inhibit the electron transfer. These CV results of step-by-step electrode modifications indicate the successful fabrication of the sensors.

3.3. Proof-of-concept detection of thrombin with CHA and TdT-mediated signal amplification

After the verification of the successful preparation of the sensing surface, DPV measurements were further utilized to investigate the responses of the sensors to the absence/presence of thrombin (1.0 nM). As depicted in Fig. 2, the incubation of the sensor with buffer shows a minimal current response at around −0.35 V (curve a) probably due to the non-specific adsorption of

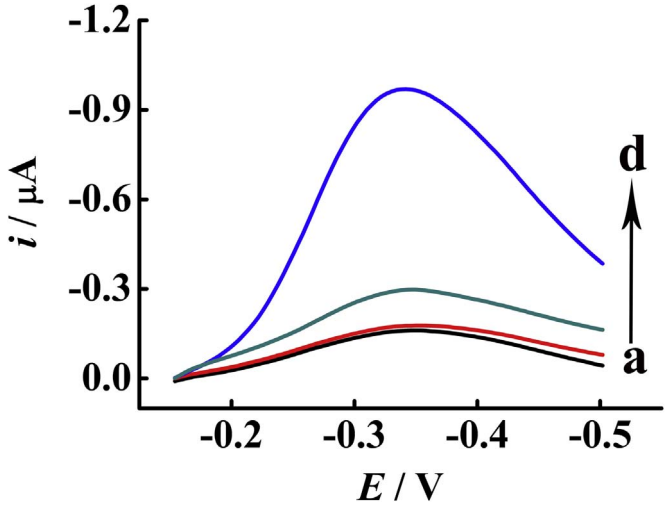

Fig. 2. DPV measurements of the T-HP/MCH/AuE sensor incubated with (a) buffer, (b) S-HP, (c) thrombin, (d) mixture of S-HP and thrombin, followed by TdT-mediated DNA polymerization and further incubation with 0.3 mM hemin for 30 min. The concentrations of T-HP, S-HP, TdT and thrombin were 0.5 μM, 1.0 μM, 1.0 U/μL and 1.0 nM, respectively. The CHA reaction time was 90 min.

hemin on the electrode. The addition of S-HP to the sensor causes negligible change in DPV peak current (curve b), indicating that S-HP is unable to hybridize with T-HP with the absence of the thrombin target. We can observe a small increase in the peak current (curve c) when the sensor is incubated with the thrombin target in the absence of S-HP. Such increase is basically due to the formation of G-quadruplex structures upon the association of T-HP with thrombin (Gloup et al., 2013). Importantly, when the sensor is incubated with the mixture of the target thrombin and S-HP, substantial increase in peak current can be obtained (curve d), owing to the formation of many G-quadruplex/hemin complexes on the sensor electrode as discussed previously. The comparison of the sensor responses to different mixtures here clearly demonstrates the significant signal enhancement capability of the sensing approach.

3.4. Optimizations for thrombin assay conditions

In order to obtain optimal sensing performance, we optimized the experimental parameters, such as the immobilization concentration of T-HP ($c_{T\text{-}HP}$), the CHA reaction time (t_{CHA}) and the incubation concentration of hemin (c_{hemin}), based on the DPV responses of the sensors to thrombin. The immobilization concentration of T-HP was first optimized in the range from 0.1 to 1.0 μM with t_{CHA} and c_{hemin} fixed at 90 min and 0.3 mM, respectively. According to Fig. 3A, the sensor shows the best signal response at 0.3 μM of $c_{T\text{-}HP}$. A lower concentration of $c_{T\text{-}HP}$ (0.1 μM) may lead to the association of less thrombin, which in turn decreases the capture of S-HP on the sensor electrode and a small current response is obtained. While, higher concentrations of $c_{T\text{-}HP}$ (above 0.3 μM) can potentially increases the steric hindrance for thrombin binding and subsequent DNA polymerization and decreased current responses are observed. Fig. 3B shows the effect of t_{CHA} on the signal response (with c_{hemin} at 0.3 mM), from which we can see that the current response gradually increases with t_{CHA} from 30 to 120 min and levels off thereafter, indicating an optimal t_{CHA} of 120 min. The effect of c_{hemin} on the sensor performance is displayed in Fig. 3C. It is obvious that the peak current elevates with increasing c_{hemin} from 0.05 to 0.2 mM and remains almost unchanged thereafter. Therefore, c_{hemin} is fixed at 0.2 mM for subsequent experiments.

3.5. Sensitivity of the aptasensor

After the experimental optimizations, the sensitivity of the developed sensor was investigated toward thrombin at different concentrations. As expected, it can be observed in Fig. 4A that the DPV response increases as the concentration of thrombin is elevated from 0 to 10.0 nM (curves a to i). Accordingly, there is a linear dependence ($R^2=0.9979$) between the peak current (i) and the logarithmic concentration of thrombin (lg c) from 0.5 pM to 10.0 nM (Fig. 4B). The linear equation is i (μA)$=3.5754+0.2598$ lg c with a detection limit of 0.12 pM based on the 3σ rule, where σ is the relative standard deviation of the blank tests (n$=11$). The performance of the developed sensor in terms of detection limit is comparable with other reported ones with complex signal amplifications and shows significant improvement over those label-free approaches for thrombin detection (Table 1). Moreover, the

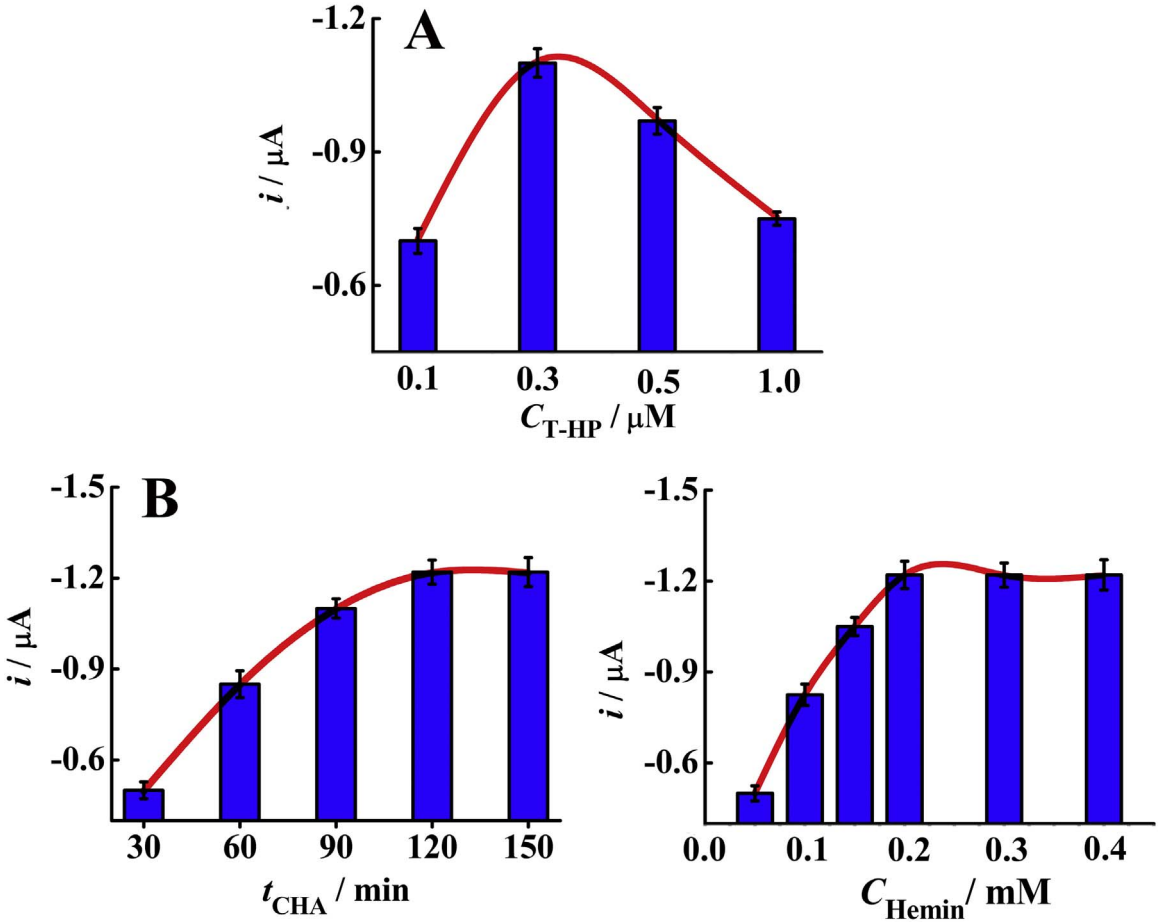

Fig. 3. The effects of (A) immobilization concentration of T-HP, (B) CHA reaction time and (C) incubation concentration of hemin on the performance of the sensor for the detection of thrombin (1.0 nM) with the presence of S-HP (1.0 μM). Error bars represented standard deviations of three parallel assays.

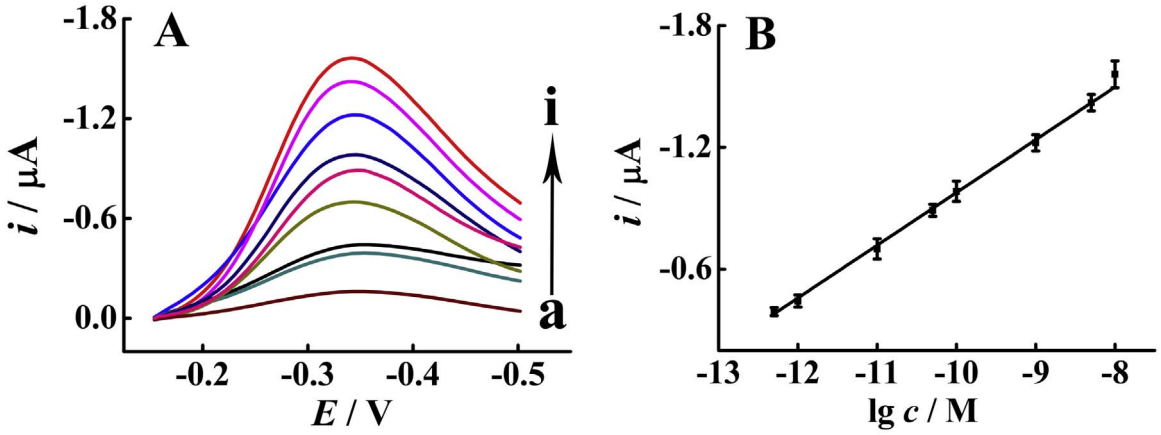

Fig. 4. (A) Typical DPV signal responses of the sensors to different concentrations of thrombin. From a to i: 0 pM, 0.5 pM, 1.0 pM, 10.0 pM, 50.0 pM, 0.1 nM, 1.0 nM, 5.0 nM, 10.0 nM. (B) Calibration curve of lg *c* vs. the peak current for thrombin in the concentration range from 0.5 pM to 10.0 nM. Error bars represented standard deviations of three parallel assays.

Table 1
Comparison of different methods for thrombin detection.

Detection method	Linear range	Detection limit	Reference
Electrochemistry	0.1 nM–200 nM	0.1 nM	Jiang et al. (2013a)
Fluorescence	5 nM–500 nM	1.1 nM	Kong et al. (2013)
Electrochemistry	0.1 nM–25 nM	0.02 nM	Zheng et al. (2015)
Electrochemistry	0.5 pM–20 nM	0.15 pM	Yuan et al. (2012)
Electrochemiluminescence	1.0 pM–5.0 nM	0.12 pM	Jie and Yuan (2012)
Electrochemiluminescence	1.0 pM–5.0 nM	0.23 pM	Wu et al. (2015a)
Electrochemistry	0.3 pM–54 pM	0.14 pM	Wang et al. (2016)
Electrochemistry	0.5 pM–10.0 nM	0.12 pM	This work

relative standard deviation evaluated by six repeated experiments with thrombin concentration at 1.0 nM is 5.8%, demonstrating a suitable repeatability of the electrochemical aptasensor.

3.6. Selectivity of the electrochemical aptasensor

In order to investigate the selectivity of the developed aptasensor to thrombin, control experiments were performed using mouse IgG (10.0 nM), lysozyme (10.0 nM) and carcinoembryonic antigen (CEA, 10.0 nM) as the interference proteins. As expected (Fig. 5), the presence of thrombin gives significant change in the DPV signal, while the presence of 10-fold excess of three other protein causes insignificant current change compared with that of the blank test (in the absence of thrombin). Besides, the mixture of the target thrombin (1.0 nM) and other three control proteins (each at 10.0 nM) shows comparable peak current to that of the presence of thrombin at 1.0 nM. These results reveal the high selectivity of the sensor platform, which is associated with the high specificity of the aptamers to the thrombin target.

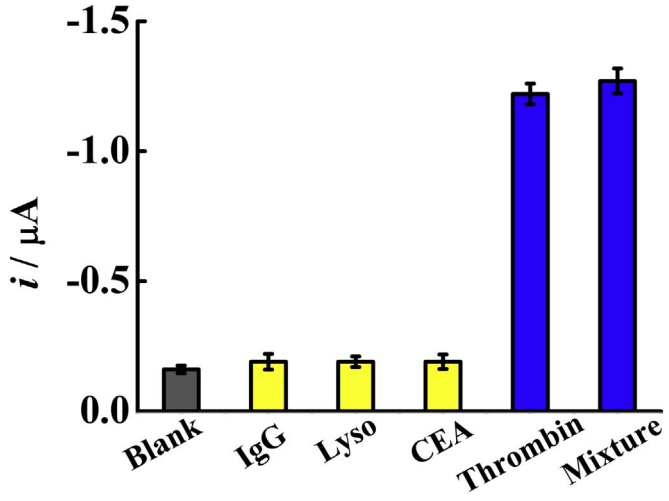

Fig. 5. Specificity investigations of the proposed aptasensor for thrombin (1.0 nM) against other non-target proteins of mouse IgG (10.0 nM), lysozyme (Lyso, 10.0 nM), carcinoembryonic antigen (CEA, 10.0 nM). Error bars represented standard deviations of three parallel assays.

3.7. The detection of thrombin in serum samples

To further evaluate the applicability of the developed aptasensor for the detection of thrombin in real samples of complicated biological matrix, we employed the standard addition method to perform recovery tests for thrombin in human serums from healthy volunteers (provided by the 9th People's Hospital of Chongqing, China). Six concentrations of thrombin (0, 1.0 pM, 10.0 pM, 50.0 pM, 1.0 nM and 5.0 nM) were added into 10-fold diluted healthy human serum samples. The results of six parallel examinations were listed in Table 2 (Note: thrombin is commonly not present in healthy human serums (Li et al., 2010), and it is undetectable with the developed method). As can be seen, the

Table 2
Recovery of thrombin in diluted human serum samples (n=6) by using the developed sensor.

Sample	Added	Found (average)	Rate of recovery (%)	RSD (%)
1	0	Undetectable	–	–
2	1.0 pM	1.01 pM	97.3–103.8	2.6
3	10.0 pM	9. 8 pM	96.6–102.6	3.1
4	50.0 pM	49.5 pM	96.9–102.8	2.7
5	1.0 nM	0.99 nM	96.8–103.5	2.2
6	5.0 nM	5.1 nM	97.7–104.1	2.9

range of the recovery for thrombin is from 96.6% to 104.1% and the relative standard deviations (RSDs) are between 2.2% and 3.1%, which indicates the applicability of the electrochemical aptasensor for monitoring thrombin in human serum samples.

4. Conclusions

We have shown the construction of a label-free and dual-amplified electrochemical sensing platform for sensitive detection of thrombin in human serum samples. The signal amplification is based on the integration of target-triggered CHA and TdT-mediated polymerization formation of G-quadruplex replicates on the sensor electrode. These G-quadruplex replicates further bind hemin and generate significantly amplified current response for detecting thrombin down to 0.12 pM. One of the major advantages of such amplified sensor design lies in the integration of two simple signal enhancement methods and completely label-free detection mode. With the advantages of high sensitivity, selectivity and simplicity, this amplified sensor strategy can be potentially employed for the monitoring of a variety of trace biomolecule targets.

Acknowledgment

This work was supported by National Natural Science Foundation of China (Nos. 21275004 and 21275119), the New Century Excellent Talent Program of MOE of China (NCET-12-0932) and Fundamental Research Funds for the Central Universities (XDJK2014A012 and XDJK2015A002).

References

Arai, T., Miklossy, J., Klegeris, A., Guo, J.P., McGeer, P.L., 2006. J. Neuropathol. Exp. Neurol. 65, 19–25.
Bauer, K.A., Rosenberg, R.D., 1984. Blood 64, 791–796.
Bock, L.C., Griffin, L.C., Latham, J.A., Vermaas, E.H., Toole, J.J., 1992. Nature 355, 564–566.
Du, J., Yue, R.R., Ren, F.F., Yao, Z.Q., Jiang, F.X., Yang, P., Du, Y.K., 2014. Biosens. Bioelectron. 53, 220–224.
Ellington, A.D., Szostak, J.W., 1990. Nature 346, 818–822.
Gao, L., Li, Q., Li, R.Q., Yan, L.R., Zhou, Y., Chen, K.P., Shi, H.X., 2015. Nanoscale 7, 10903–10907.
Gloup, E., Freeman, R., Willner, I., 2013. Anal. Chem. 85, 12126–12133.
Guo, Y.H., Wu, J., Ju, H.X., 2015. Chem. Sci. 6, 4318–4323.
Huang, Y., Chen, J., Zhao, S.L., Shi, M., Chen, Z.F., Liang, H., 2013. Anal. Chem. 85, 4423–4430.
Huang, Y., Liu, X.Q., Huang, H.K., Qin, J., Zhang, L.L., Zhao, S.L., Chen, Z.F., Liang, H., 2015. Anal. Chem. 87, 8107–8114.
Jiang, B.Y., Wang, M., Li, C., Xie, J.Q., 2013a. Biosens. Bioelectron. 43, 289–292.
Jiang, F.X., Yue, R.R., Du, Y.K., Xu, J.K., Yang, P., 2013b. Biosens. Bioelectron. 44, 127–131.
Jie, G.F., Yuan, J.X., 2012. Anal. Chem. 84, 2811–2817.
Jin, G.X., Wang, C.M., Yang, L.L., Li, X.J., Guo, L.H., Qiu, B., Lin, Z.Y., Chen, G.N., 2015. Biosens. Bioelectron. 63, 166–171.
Kong, L., Xu, J., Xu, Y.Y., Xiang, Y., Yuan, R., Chai, Y.Q., 2013. Biosens. Bioelectron. 42, 193–197.
Li, B.L., Ellington, A.D., Chen, X., 2011. Nucleic Acids Res. 39, e110.
Li, F., Zhang, H.Q., Wang, Z.X., Li, X.K., Li, X.F., Le, X.C., 2013. J. Am. Chem. Soc. 135, 2443–2446.
Li, L.D., Zhao, H.T., Chen, Z.B., Mu, X.J., Guo, L., 2010. Anal. Bioanal. Chem. 398, 563–570.
Liu, H.Y., Xu, S.M., He, Z.M., Deng, A.P., Zhu, J.J., 2013. Anal. Chem. 85, 3385–3392.
Liu, Z.L., Li, W., Nie, Z., Peng, F.F., Huang, Y., Yao, S.Z., 2014. Chem. Commun. 50, 6875–6878.
Lu, C.H., Willner, I., 2015. Angew. Chem. Int. Ed. 54, 12212–12235.
Mei, H.C., Bing, T., Qi, C., Zhang, N., Liu, X.J., Chang, T.J., Yan, J.L., Shangguan, D.H., 2013. Chem. Commun. 49, 164–166.
Pabinger, I., Ay, C., 2009. Arterioscler. Thromb. Vasc. Biol. 29, 332–336.
Qian, Y., Gao, F.L., Du, L.L., Zhang, Y., Tang, D.Q., Yang, D.Z., 2015. Biosens. Bioelectron. 74, 483–490.
Tjing, V., Yu, H., Hucknall, A., Rangarajan, S., Chilkoti, A., 2011. Anal. Chem. 83, 5153–5159.
Tuerk, C., Gold, L., 1990. Science 249, 505–510.
Wang, C.Q., Du, J., Wang, H.W., Zou, C.E., Jiang, F.X., Yang, P., Du, Y.K., 2014. Sens. Actuator B – Chem. 204, 302–309.
Wang, Y.G., Zhang, Y., Yan, T., Fan, D.W., Du, B., Ma, H.M., Wei, Q., 2016. Biosens. Bioelectron. 80, 640–646.
Wu, D., Xin, X., Pang, X.H., Pietraszkiewicz, M., Hozyst, R., Sun, X.G., Wei, Q., 2015a. ACS Appl. Mater. Interfaces 7, 12663–12670.
Wu, H., Zhang, K., Liu, Y.L., Wang, H.Y., Wu, J., Zhu, F.F., Zou, P., 2015b. Biosens. Bioelectron. 64, 572–578.
Xia, H., Li, L.L., Yin, Z.Y., Hou, X.D., Zhu, J.J., 2015. ACS Appl. Mater. Interfaces 7, 696–703.
Xu, Y.Y., Xu, J., Xiang, Y., Yuan, R., Chai, Y.Q., 2014. Biosens. Bioelectron. 51, 293–296.
Yang, B., Zhang, X.B., Kang, L.P., Shen, G.L., Yu, R.Q., Tan, W.H., 2013. Anal. Chem. 85, 11518–11523.
Yang, C.Y., Shi, K., Dou, B.T., Xiang, Y., Chai, Y.Q., Yuan, R., 2015. ACS Appl. Mater. Interfaces 7, 1188–1193.
Yang, L.T., Ellington, A.D., 2008. Anal. Biochem. 380, 164–173.
Yu, P., Zhang, X.H., Xiong, E.H., Zhou, J.W., Li, X.Y., Chen, J.H., 2016. Biosens. Bioelectron. 85, 471–478.
Yuan, Y.L., Yuan, R., Chai, Y.Q., Zhuo, Y., Ye, X.Y., Gan, X.X., Bai, L.J., 2012. Chem. Commun. 48, 4621–4623.
Zhang, H.F., Shuang, S.M., Sun, L.L., Chen, A.J., Qin, Y., Dong, C., 2014. Microchim. Acta 181, 189–196.
Zhao, Q., Gao, J., 2013. Chem. Commun. 49, 7720–7722.
Zheng, Y.N., Yuan, Y.L., Chai, Y.Q., Yuan, R., 2015. Biosens. Bioelectron. 66, 585–589.
Zuker, M., 2003. Nucleic Acids Res. 31, 3406–3415.